JOURNAL OF GEOPHYSICAL RESEARCH, VOL. 87, NO. B4, PAGES 2840-2850, APRIL 10, 1982

GLOBAL Q ESTIMATES FROM ANTIPODAL RAYLEIGH WAVES

Eric P. Chael and Don L. Anderson

Seismological Laboratory, California Institute of Technology
Pasadena, California 91125

Abstract. Global average estimates of the group velocity and attenuation of long-period (120-300 s) Rayleigh waves were made using seismograms from the epicenter's antipode ($\Delta \simeq 180^{\circ}$). Focusing at the antipode produced amplified arrivals with favorable signal-to-noise ratios. The high-quality data yielded very stable attenuation values, with excellent agreement between the results from successive Rayleigh arrivals for a single event and between the results for two different events. Lateral heterogeneities in earth structure can cause systematic biasing of attenuation measurements based on antipodal records. The initial, uncorrected results therefore provide a lower bound estimate of global Q. An ellipsoidal perturbation in shape was used to simulate the effects of lateral velocity heterogeneities on Rayleigh wave propagation. Using the agreement of repeated attenuation measurements as a constraint, we estimated both the bias in those measurements and the splitting widths of the Rayleigh modes. At a period of 200 s, the estimated splitting width is 0.30%; this agrees closely with calculations by Luh (1974) for an earth model with different continental and oceanic velocity profiles. The estimated bias varied from 30% to zero over the 120- to 260-s band. After correcting for bias, the antipodal Q values range from 108 at 120 s to 188 at 260 s. These Q are within the range of previous measurements but are lower than the mean values from typical great circle studies, implying that the globally averaged upper mantle is slightly more attenuative than has been generally recognized.

Introduction

Fundamental mode Rayleigh surface waves have long been employed in the study of upper mantle attenuation. Most such studies [e.g., Kanamori, 1970; Mills and Hales, 1977, 1978; Nakanishi, 1979] have involved measuring the spectral decay of successive group arrivals (R2-R4, R3-R5, etc.) at a variety of stations. The values calculated from a particular record are interpreted as representative of the great circle connecting the epicenter and station; Rayleigh wave attenuation values appropriate as global averages are then determined by combining the results for many distinct great circles.

We have obtained a more direct measure of average global attenuation through the analysis of recordings from the antipodal regions of two earthquakes. Because the antipode is a caustic for Rayleigh wave propagation, it offers two immediate advantages. First, energy arriving from all azimuths, i.e., energy that has sampled the entire globe, contributes to the antipodal record. Such a record thus reflects average global properties rather than the structure along a particular great circle. Global averages can therefore be obtained from a single event at a single station. The earth does the averaging; combining different events and stations, with the attendant accumulation of errors, is not necessary. Second, if the arriving energy is consistent in phase, constructive interference produces strong amplification of the signal, reducing the effect of noise contamination. Both advantages are clearly dependent on the radiation pattern of the event. An isotropic explosion, for example, radiates equal energy with uniform phase at all azimuths, yielding at the antipode of a spherically symmetric globe complete constructive interference for vertical motion, and complete cancellation of horizontal motion. Of the shear dislocation sources, a shallow, 45° dip slip event is most favorable. The Rayleigh wave radiation pattern of such an event has two wide phase-symmetric lobes, offering the greatest degree of constructive interference at the antipode.

In a sense, the earth behaves as a giant lens, bringing all of the Rayleigh wave energy from an earthquake to a focus at the antipode. Many other wave modes have a caustic at the antipode as well, but we treat here only the fundamental Rayleigh wave. Dispersion of the wave train, analogous to a chromatic aberration of the lens, smears out the temporal focusing. The spatial focusing is degraded by lateral heterogeneities in the earth's velocity structure, which represent imperfections in the figure of the lens. By examining the quality of the focusing near the antipode, we have been able to constrain the effects of lateral heterogeneities on a portion of the Rayleigh wave spectrum. This information should in turn constrain the nature of such heterogeneities in the earth's upper mantle; specifically, it may indicate the extent to which continental and oceanic structures differ.

Stacking seismograms has been a common procedure for increasing signal-to-noise in studies of mantle Q [Jordan and Sipkin, 1977; Sailor and Dziewonski, 1978]. It is well known that the Q estimated from stacks is biased toward low values. On the other hand the records which go into the stack are either selected on the basis of high signal-to-noise or represent a indiscriminate sampling of available records. It is therefore difficult to estimate the net bias of the resulting Q measurements or even to determine its sign since the unavailable or discarded data is not included in the analysis. Previous estimates of average mantle attenuation involve a sparse and non-uniform sampling. In contrast to this the antipodal experiment involves a uniform sampling, weighted by the radiation pattern. The

Paper number 2B0176.
0148-0227/82/002B-0176$05.00

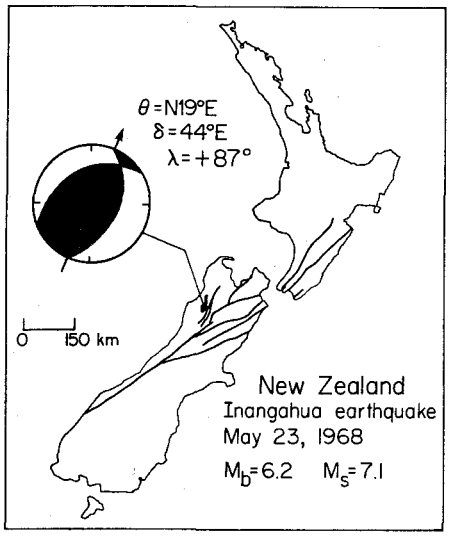

Fig. 1. Location and focal mechanism (lower hemisphere projection) of the Inangahua, New Zealand, earthquake of May 23, 1968. The earthquake occurred on the Glasgow Fault, a branch of the Alpine-Wairau system.

low-Q paths are automatically included in the 'stack'. Lateral heterogeneities in velocity cause imperfect constructive interference at the antipode, which introduces some bias. A unique aspect of the antipodal method is that the sign of the bias is known. We therefore have an upper bound on global attenuation (or a lower bound on Q). Antipodal estimates are thus a useful complement to conventional surface wave and free oscillation measurements of Q even if the magnitude of the bias cannot be estimated precisely. Because of the intrinsic advantages of the natural earth 'stack' we have made an effort to estimate the bias. This is not possible in conventional experiments because of the missing data.

Data Analysis

Our best antipodal data were from a seismogram of the Inangahua, New Zealand, earthquake of May 23, 1968 (M_s=7.1, latitude=41.72°S, longitude=172.03°E, h=21 km, time=1724:17 (ISC)), recorded at WWSSN station PTO (Porto, Portugal; latitude=41.14°N, longitude=8.60°W). The body waves on this record have been previously studied by Rial [1978a, b]. Focal mechanism studies reveal this event to have been of predominantly thrust type [Robinson et al., 1975] (see Figure 1), satisfying the need for constructive interference of the Rayleigh lobes at the antipode. The station lies at a distance of 179.25° from the epicenter, or about 80 km from the true antipode, assuming a spherical earth of radius 6371 km. The wavelengths of the long period (120-300 s) waves analyzed here vary from about 500 to 1600 km, so PTO is for these periods only a fraction of a wavelength from the antipode. As a result, we expected the seismogram to exhibit the features of a true antipodal recording.

The long-period vertical record from PTO was digitized and interpolated to a sampling interval of 2 s. The first three Rayleigh wave arrivals were then extracted using conservative group velocity windows covering roughly 2.7 to 4.4 km/s. Because at the antipode the conventionally labeled arrivals R1 and R2 overlap, the first Rayleigh arrival will be referred to as R1R2; similarly, the second is called R3R4 and the third, R5R6. These arrivals correspond to propagation distances of 180°, 360°+180°, and 2x360°+180°, respectively.

Each window was then convolved with a

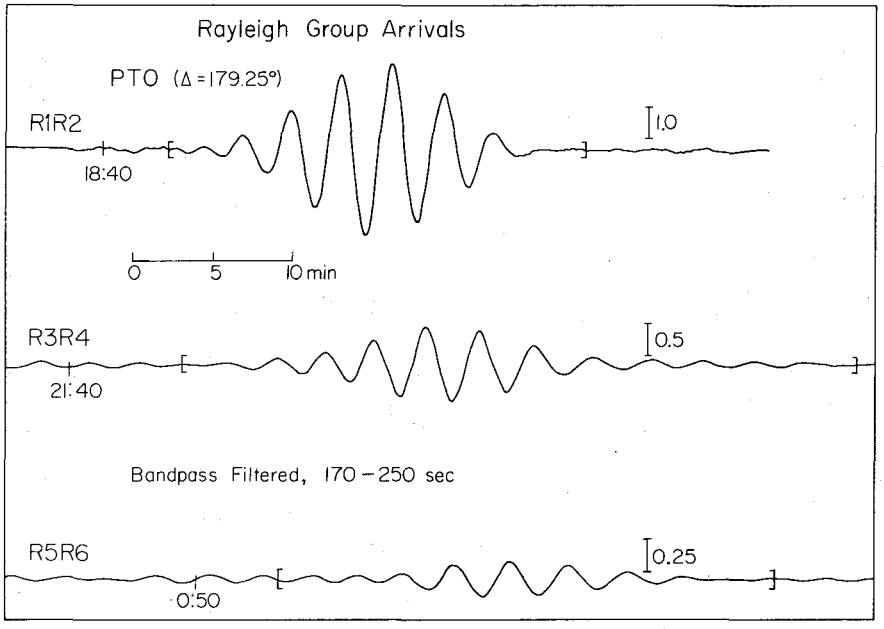

Fig. 2. Band-pass-filtered vertical component records of the first three Rayleigh wave arrivals at the antipodal station PTO. Note changes in amplitude scales. Arrivals were windowed between the brackets, then Fourier-transformed in order to obtain spectral amplitude ratios. This process was repeated for several filter bands in the 120- to 300-s period range.

succession of narrow-band filters of the form

$$H(t) = \frac{\delta}{2\sqrt{\pi}} \cos(\omega_0 t)\exp(-\delta^2 t^2/4)$$

where

δ = filter half-width, equal to $(\omega_1 - \omega_2)/2$;
ω_0 = central frequency, equal to $(\omega_1 + \omega_2)/2$;
ω_1 = high-frequency cutoff;
ω_2 = low-frequency cutoff.

Best results were obtained for a filter half-width δ of 10 mHz; 10 different filters were used, spanning the 120- to 300-s period range. In most cases, the filtered traces exhibited well-defined, dispersed wave groups. Some representative examples are shown in Figure 2. Group velocities were calculated from the peak amplitude time of each filtered wave group using the formula

$$U(\omega) = (t_p(\omega) - t_0)/\Delta$$

where

$t_p(\omega)$ = peak amplitude time of group with central frequency ω;
t_0 = origin time of event;
Δ = propagation distance.

Here, the propagation distance Δ was based on a mean earth circumference of 40,030 km, and the assumption that the station lies at the true antipode. No corrections were made for source or instrumental group delay times. Following Kanamori and Abe [1968], we estimated these combined corrections to be no greater than 0.7% of the travel time of the first (R1R2) arrival.

Figure 3 shows the group velocity values, together with the global average values given by Mills and Hales [1977]. These authors used a least squares parabola-fitting technique to determine group velocities for many great circle paths. Their results were very well constrained and showed little deviation between paths. The excellent agreement (generally within 0.01 km/s or 0.3%) of our results with Mills and Hales' values convinced us that PTO was located near enough to

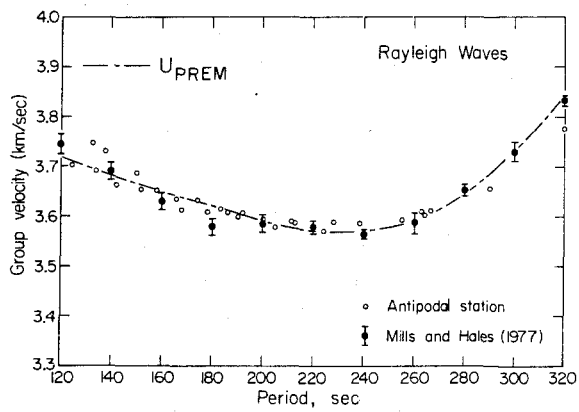

Fig. 3. Rayleigh wave group velocity measurements obtained from the PTO record. Also shown are Mills and Hales' [1977] average values of many great circle paths and the dispersion curve for the preliminary reference earth model (PREM) of Dziewonski and Anderson [1981].

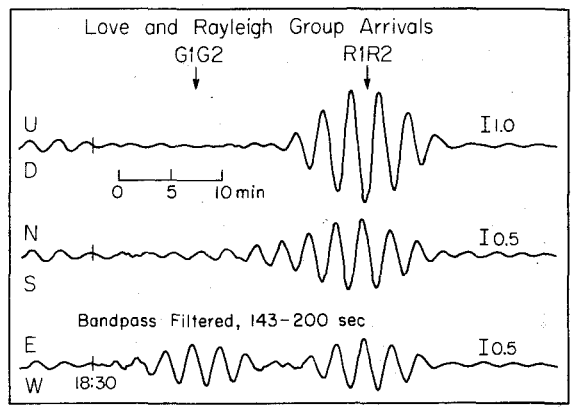

Fig. 4. Filtered records of the three components of motion at PTO, showing the first Love (G1G2) and Rayleigh (R1R2) arrivals. Note that the Love wave is strongest on the E-W component, while the N-S and E-W Rayleigh components are of comparable strength.

the geometric antipode and that the focusing there was sufficiently sharp to suit our purpose of measuring global average attenuation.

The three-dimensional ground motion of the R1R2 arrival at PTO also testifies to the sharpness of focusing at the antipode. The three components of the observed R1R2 motion, filtered for 143- to 200-s energy, are shown in Figure 4. These waveforms were combined to produce the seismoscope-style plots of Figure 5. If the earth were spherically symmetric and the event a point source, the expected ground motion would be a plane-polarized ellipse. In that case, the Rayleigh motion would yield a line in Figures 5a and 5c and a somewhat narrower ellipse than that in Figure 5b. Source finiteness, contamination by other modes, random noise, and lateral heterogeneities in earth structure all act to degrade the ideal polarization. Yet, as Figure 5 shows, the actual ground motion recorded at PTO is very strongly polarized. This well-defined Rayleigh polarization at the antipode, where energy is arriving from all azimuths, dramatically demonstrates the high quality of the 'earth lens.' Notice on the horizontal projection (Figure 5a) that the Love (G1G2) and Rayleigh (R1R2) arrivals are not polarized perpendicularly to each other. This unusual phenomenon is actually expected in the antipodal region, where the transverse spheroidal and longitudinal toroidal components become significant, rotating the Rayleigh and Love polarization directions.

To measure the attenuation, the prominent Rayleigh wave groups were extracted from the broad-windowed, narrow-band-filtered traces. This was essentially equivalent to restricting the time windows to a group velocity range appropriate for the pass band of each filter. In this way it was possible to remove from the signals energy outside of the wave groups but perhaps within the originally wide arrival windows. Each wave group was padded with zeroes to a length of 4096 samples and transformed to the frequency domain by using a standard FFT routine. No smoothing of the resulting amplitude spectra was considered necessary. The attenuation coefficient $\gamma(T)$ was calculated from

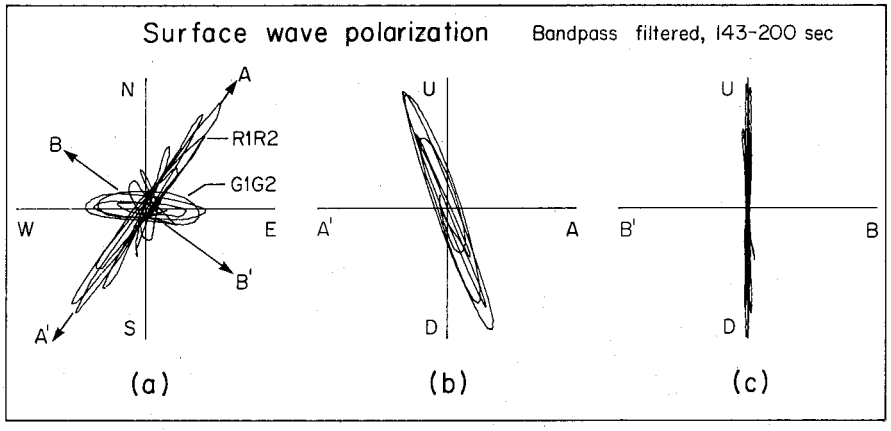

Fig. 5. Two-dimensional projections of the filtered ground motions at PTO made by combining the traces of Figure 4. For each projection, the two axes are scaled the same, but the scaling differs between projections. Note on the horizontal projection of Figure 5a that the G1G2 and R1R2 arrivals are not perpendicularly polarized. Figures 5b and 5c are vertical projections along A-A′ and B-B′, respectively, of Figure 5a, without the G1G2 arrival. The R1R2 motion is strongly polarized in a vertical plane.

$$\gamma(T) = \frac{\ln[A_i(T)/A_j(T)]}{\Delta_j - \Delta_i}$$

where $A_i(T)$ is the spectral amplitude at period T of the ith arrival and Δ_i is the propagation distance of the ith arrival. This attenuation coefficient is related to the quality factor Q through the relation

$$Q(T) = \frac{\pi}{T\gamma(T)U(T)}$$

Values of γ were determined at several frequency points across the band of each of the filters; the considerable overlap in the frequency response of successive filters resulted in redundant measurements at each frequency, the spread of which indicates the effects of noise and our windowing methods. By measuring the decay between both the first and second (R1R2/R3R4) and first and third (R1R2/R5R6) arrivals, we made two essentially independent determinations of $\gamma(T)$. In Figure 6, we have plotted $\gamma(T)$ values from the PTO record together with representative values of Mills and Hales [1977]. The error bars ($\pm 1\sigma$) on their results typify the scatter seen in great circle studies not only between different great circles but also for repeated measurements along a single one. At periods less than 200 s our results fall outside the $\pm 1\sigma$ error bars of Mills and Hales [1977] but within the total scatter of their data. This scatter may result from lateral refractions of the propagating Rayleigh wave, contamination of the signal by overtone energy, or poor signal-to-noise ratios. In contrast, our values display a very smooth, stable trend, indicating that amplification at the antipode has significantly improved the signal level. Our results also exhibit excellent consistency between the R1R2/R3R4 and R1R2/R5R6 measurements. This consistency immediately confirms that the windowed Rayleigh arrivals are sufficiently isolated from significant overtone energy. In a later section, this consistency will be used as a constraint on the possible bias induced by a laterally heterogeneous velocity structure.

Before we can assert that our attenuation values represent global averages, we must consider how the radiation pattern of the Inangahua event affected the sampling of the mantle. Rial [1978b], studying the body waves, modeled the earthquake as a triple event. The three sources shared a common epicenter and focal mechanism (strike=19°, dip=44°, rake=+87°) but differed in depth, seismic moment, and origin time. For long-period Rayleigh waves, these differences are inconsequential, and Rial's triple source can be portrayed as a single event. The Rayleigh wave radiation pattern for this event displays the double-lobed nature typical of a thrust event. Assuming the earth was well sampled between the

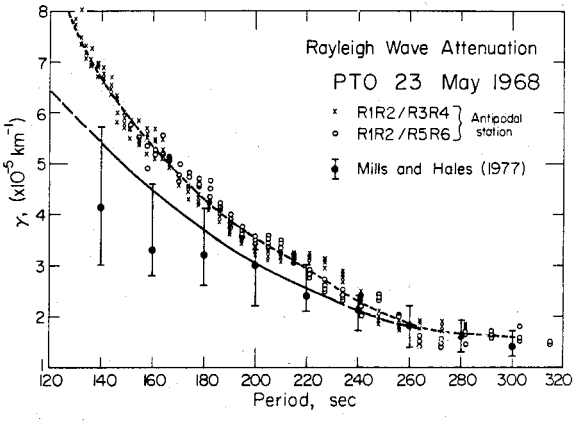

Fig. 6. Values of the attenuation coefficient γ as a function of period, obtained from the PTO record. The use of several band-pass filters with considerable overlap resulted in multiple values at each period. Note both the small amount of scatter and the consistency of the R1R2/R3R4 and R1R2/R5R6 trends. The dashed line follows the smoothed average trend of the measurements. The solid line beneath the measured values from 140 to 240 s represents the best estimate of average γ after correcting for possible bias.

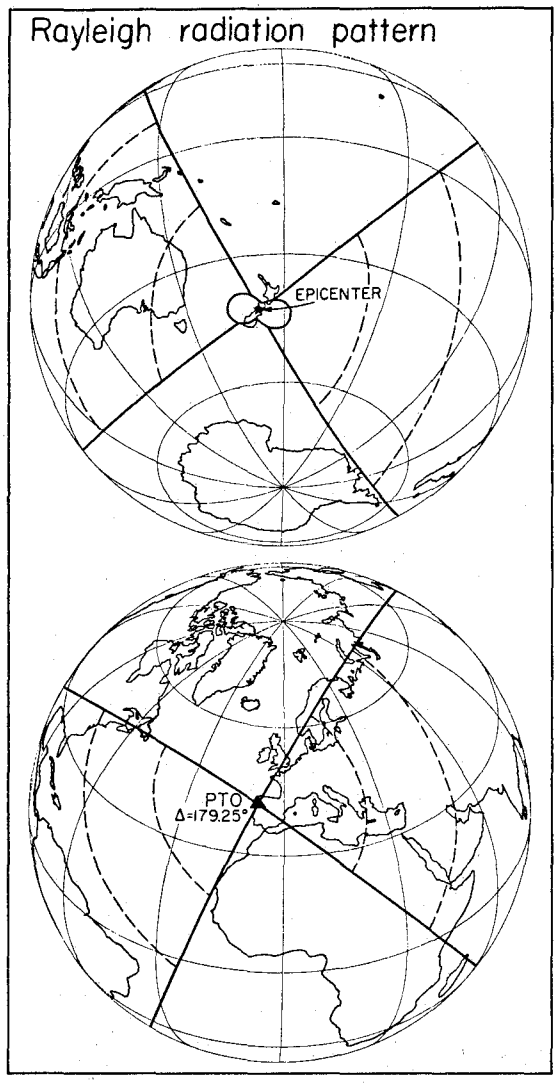

Fig. 7. Global projection of the Rayleigh wave radiation pattern of the Inangahua earthquake. The top figure shows the long-period radiation pattern overlying the epicenter. The heavy solid lines are the great circles through the half-maximum amplitude directions of the radiation pattern. The dashed lines indicate the regions most strongly sampled.

half amplitude azimuths of the lobes, we realized a coverage range of about 200°, greater than half of the globe. Figure 7 shows the radiation pattern superimposed on the epicenter, with great circles drawn through the half-amplitude points. Because the preferentially sampled zone includes a representative distribution of oceanic, continental, and tectonic regions, the PTO results should reflect an accurate measure of average global attenuation.

A second antipodal recording was produced by an intermediate depth South American earthquake on February 21, 1971, centered near the junction of Chile, Argentina, and Bolivia (M_S=6.8, latitude=23.81°S, longitude=67.20°W, h=166 km, time=1035:20 (ISC)). The WWSSN station HKC in Hong Kong (latitude=22.30°N, longitude=114.17°E) falls at an epicentral distance of 178.05°, putting it within half a wavelength of the antipode for 120 s and longer Rayleigh waves. The long-period vertical record was processed in the manner described above. The Rayleigh waves were weaker on this record than on the PTO record due to the depth and size of the event, so we could only use the first two arrivals (R1R2 and R3R4).

The attenuation coefficients determined from these arrivals are shown in Figure 8. The values are in good agreement with those obtained from the PTO record, especially at periods shorter than 220 s. The source-station orientation on the globe for this second event was totally different from that for the first, resulting in a much different sampling of the earth by this event's radiation pattern. Yet the attenuation values measured in both cases were virtually identical. This agreement strongly implies that in each case the sampling of the earth was sufficient to reveal global average properties. Also, any biasing due to lateral heterogeneities must be similar for the two events.

Possible Bias

Various investigators [e.g., Dahlen, 1979a, b; Sleep et al., 1981] have suggested that the earth's lateral heterogeneities may systematically bias measurements of attenuation. This is because a general aspherical perturbation in the structure of the earth removes the 2ℓ+1-fold degeneracy in eigenfrequency of the singlets ${}_nS_\ell^m$ comprising the normal mode peak ${}_nS_\ell$. If this splitting of the singlets is of the same order as the attenuative broadening, it will be unresolvable; it will act to broaden further the overall peak shape. If naively assumed to be unsplit, the peak would then be interpreted as having an erroneously low Q. The initial results therefore provide lower-bound estimates of the global Q for Rayleigh waves. Dahlen [1979a, b] argues that the bias should be insignificant for conventional single-station analyses, while attenuation measurements based on stacked or antipodal records may be strongly biased toward lower Q. Our antipodal observations do in fact yield lower Q at periods below 240 s than many great circle studies. Averages from these conventional great circle determinations may be biased as well, though for a different reason.

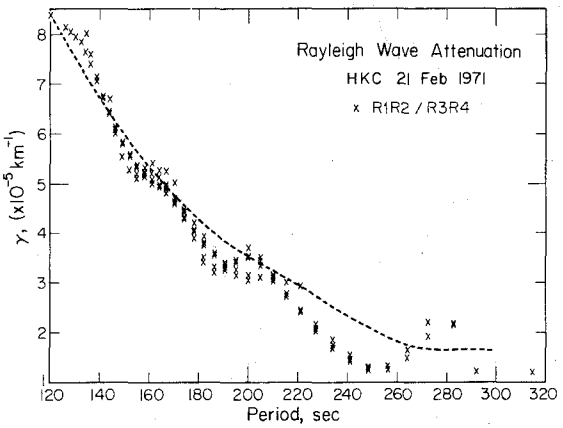

Fig. 8. Values of the attenuation coefficient γ obtained from the HKC record of a South American event (Δ=178.05). The dashed line gives the smoothed average trend of the measurements from the PTO record (Figure 6).

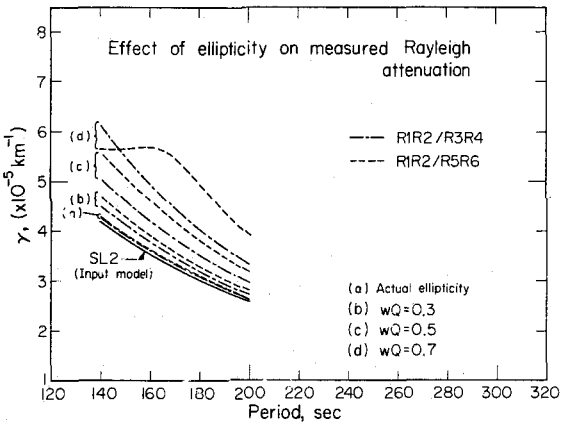

Fig. 9. Effect of ellipticity on measurements made near the antipode of the attenuation coefficient γ. Synthetic Rayleigh arrivals were generated for an ellipsoidal earth model using attenuation model SL2 of Anderson and Hart [1978]. Attenuation values measured from the synthetic arrivals show greater bias from the SL2 curve as the ellipticity increases (increasing wQ). As the bias increases, so does the separation of the 'measured' R1R2/R3R4 and R1R2/R5R6 curves. Note that the bias induced by the earth's actual ellipticity is negligible.

In this case, a representative number of low-Q paths may not be included in the averages because of the low amplitudes of the later arrivals. In the antipodal case all great circle paths are automatically included in the average. To estimate the bias in our measurements and get at the actual intrinsic attenuation, we sought to account for the effects of lateral heterogeneities.

Method

To put limits on the possible bias in our attenuation measurements, we represent lateral heterogeneity as an ellipsoidal perturbation in shape. For 120- to 300-s periods, the earth's actual ellipticity ($f \simeq 1/298$) has a negligible effect, as shown in Figure 9. We examine the effects of an exaggerated ellipticity: the regular azimuthal variation in great circle path length on the ellipsoid replaces the real situation of an irregular azimuthal distribution of great circle average group velocity. Velocity perturbations can be modeled as path length perturbations since both cause travel times to the antipode to be path dependent, so that the constructive interference there of energy arriving from different azimuths is degraded. Because the splitting caused by the real earth is unresolvable, we are not interested in the specific frequencies and amplitudes of the singlets under a particular peak. Rather, we are concerned only with the character of the resultant peak itself and with any side effects that the splitting may have on the time domain signals. Thus, we attempt to order the singlets using an elliptical heterogeneity and 'statistically' imitate the mode peaks produced by the earth's velocity heterogeneities. We seek, in particular, an observable side effect which could be used to constrain the amount of splitting (and hence the bias in antipodal attenuation measurements) caused by the real earth. Previous attempts to obtain global attenuation by averaging or stacking can be considered sparse and incomplete averages or stacks with no estimate of bias possible.

Theory

Following the treatment given by Dahlen [1979b], let $u(\underline{r},\omega)$ represent the spectrum of the radial component of the fundamental mode Rayleigh wave at $\underline{r}$ on an ellipsoidal, nonrotating earth due to a source at $\underline{r}_s$. To first order in the eigenfrequencies and zeroth order in the eigenfunctions, this spectrum can be expressed as

$$u(\underline{r},\omega) = \sum_{\ell=0}^{\infty} \sum_{m=0}^{\ell} A_\ell^m(\underline{r}) c_\ell^m(\omega) \qquad (1)$$

The amplitude term A_ℓ^m is a rather complicated combination of the source moment tensor elements, the displacement scalars U and V, and factors determined by the source and station locations. Complete expressions for A_ℓ^m can be found in the work by Dahlen [1979b]. Spectra of the two horizontal components are given by formulas identical to (1), with somewhat different expressions for the amplitude terms. The term $c_\ell^m(\omega)$ defines the spectral shape of a singlet peak

$$c_\ell^m(\omega) = -\tfrac{1}{2}\left[\alpha_\ell + i(\omega-\omega_\ell^m)\right]^{-1} - \tfrac{1}{2}\left[\alpha_\ell + i(\omega+\omega_\ell^m)\right]^{-1} \qquad (2)$$

The eigenfrequencies ω_ℓ^m of an ellipsoidal earth are given by

$$\omega_\ell^m = \omega_\ell^d\left[1 + a_\ell\left(1 - \frac{3m^2}{\ell(\ell+1)}\right)\right] \qquad (3)$$

where ω_ℓ^d is the degenerate eigenfrequency for a spherically symmetric earth. The splitting of the eigenfrequencies is determined by the single parameter a_ℓ, which is proportional to the ellipticity. Defining w_ℓ as the (dimensionless) total splitting width $w_\ell = (\omega_\ell^0 - \omega_\ell^\ell)/\omega_\ell^d$, one finds from (3) that $w_\ell \simeq 3a_\ell$ (for $\ell \gg 1$). The eigenfrequencies given by (3) are doubly degenerate, i.e., $\omega_\ell^{-m} = \omega_\ell^m$; this fact has been incorporated into (1). The ellipsoidal perturbation alters the spherically symmetric spectra only through the frequency shifts of the singlet peaks. The singlet amplitudes A_ℓ^m are unaffected by the ellipticity. Transforming (1) into the time domain yields

$$u(\underline{r},t) = -\sum_{\ell=0}^{\infty} \sum_{m=0}^{\ell} A_\ell^m(\underline{r}) \exp(-\alpha_\ell t)\cos(\omega_\ell^m t) \qquad (4)$$

The above treatment assumes the attenuation to be laterally homogeneous. More realistically, each singlet should have a distinct value, α_ℓ^m, as its decay rate. If the excitation of the singlets is sufficiently uniform, as it should be for antipodal stations, then the width of the composite peak, neglecting splitting, would be the average of the singlet widths. In this case it is reasonable in the modeling procedure to replace the distinct values α_ℓ^m by the average value α_ℓ. The corresponding average Q can be obtained from

$Q_\ell=\omega_\ell^d/2\alpha_\ell$. This is just another way of saying that the antipode acts as a natural averager of global attenuation, assuming there is sufficiently complete sampling of the globe by the event's radiation pattern. The fact that the results from two different events agree so closely (Figures 6 and 8) argues in favor of sufficient sampling.

Again, let us emphasize that we are not concerned with the earth's actual ellipticity of figure; we use an elliptical earth model to simulate the effects of lateral heterogeneities in the earth's elastic parameters. Because of this, we are free to locate the event anywhere on the ellipsoid. Furthermore, we can orient the strike of the fault plane as desired. The receiver is then located at the proper distance from the event along the azimuth appropriately oriented relative to the event strike. To model the PTO records of the Inangahua event, we have used

$$\text{Distance}=179.15^\circ$$
$$\text{Azimuth}=\text{Strike}+140.0^\circ.$$

(We took the liberty of slightly relocating the event in order to match more accurately the observed ratio of horizontal to vertical amplitudes and the direction of the horizontal polarization of the R1R2 arrival. The discrepancies that resulted from using the event location as given earlier (in which case Distance=179.25° and Azimuth=Strike+121.6°) are slight, and probably due as much to inaccuracies in the earth model and source mechanism employed as to a real error in event location.)

Synthetic time domain Rayleigh waves were generated by a program based on (3) and (4), using earth model 1066A of Gilbert and Dziewonski [1975] and Q model SL2 of Anderson and Hart [1978]. The synthetic Rayleigh arrivals were convolved first with an instrument operator, and then with a 143- to 200-s narrow-band filter as used in the analysis of the real data. As suggested by Dahlen [1979b], the splitting parameter a_ℓ was chosen to vary with ℓ such that the product $w_\ell Q_\ell$ remained constant. The 120- to 300-s period range involves orders ℓ of roughly 80 to 25. Since Q decreases with increasing ℓ in this range, the condition $w_\ell Q_\ell$=const means that w_ℓ increases for shorter periods. This, in turn, means that for shorter periods the ellipticity becomes greater, so that the modeled earth was, like the real earth, increasingly heterogeneous at shorter wavelengths. Other recipes for w_ℓ could be devised, such as a more general power law model, e.g., $w=kQ^{-\eta}$. Since the splitting should not change drastically over a narrow bandwidth and all our synthetics were narrow-band filtered, the splitting effects displayed by the synthetics would not be sensitive to the specific recipe employed.

Estimating the Bias

We used the consistency of the R1R2/R3R4 and R1R2/R5R6 measurements to estimate the bias in the antipodal attenuation values. From a time domain perspective, the lateral heterogeneities act to degrade the constructive interference at the antipode, so that the signal amplification will decrease for each successive Rayleigh arrival. This reduction in amplification is a nonlinear function of the phase mismatch of the energy approaching the antipode from different azimuths. One might thus expect the R1R2/R5R6 attenuation values to be biased somewhat more than the R1R2/R3R4 values. We examined this argument by generating synthetics of the first three Rayleigh arrivals at PTO, for various values of the splitting factor wQ, and then measuring the apparent attenuation between the three arrivals. We determined that the agreement of the R1R2/R3R4 and R1R2/R5R6 attenuation values can be used to estimate the amount of bias in those values caused by lateral heterogeneities and that this estimate can be reasonably established by representing the heterogeneities as a simple ellipsoidal perturbation.

Figure 9 was produced with the source on the equator of the ellipsoid. Notice in Figure 9 that, as the bias from the input attenuation curve increases, so does the separation of the R1R2/R3R4 and R1R2/R5R6 'measured' curves. For sufficiently large wQ the usual trend of a curve toward greater bias at shorter periods would reverse. This is seen in Figure 9 on the R1R2/R5R6 curve for wQ=0.7, below 160 s. This occurred because the range in path lengths with azimuth for the R5R6 arrival exceeded half a wavelength. The separation of the R1R2/R3R4 and R1R2/R5R6 curves is decreased only over a very narrow period band. It was not possible to obtain both large bias and small separation of the two curves across the full 143- to 200-s band. The behavior of the curves in Figure 9 was found to be independent of the source-station orientation on the ellipsoid. For wQ=0.7, the synthetic R1R2/R3R4 and R1R2/R5R6 curves are separated much more than the observed trends plotted in Figure 6. Thus the bias in the observed measurements must be less than the difference shown in Figure 9 between the SL2 curve and the curves for wQ=0.7. We should mention here that, at a fixed period T, it is the differences γ(R1R2/R5R6) - γ(R1R2/R3R4) and γ(R1R2/R3R4) - γ(input) which are important, and these are strictly determined by the value of the splitting width w. The shifts between the curves are independent of the specific input attenuation model. We feel that the separation of the two curves which was produced using wQ=0.5 represents a reasonable upper limit to the observed separation. The amount by which the synthetic 'measured' curves are shifted above the input Q model for wQ=0.5 is thus our best estimate of the amount by which the observed attenuation values can be biased from the actual intrinsic attenuation. Subtracting this amount of bias from the observed values, we obtained the solid curve in Figure 6. This corrected curve establishes the best estimate of average global attenuation consistent with our antipodal measurements. At periods below 150 s, the R5R6 signal fell into the noise, so that we could not determine stable R1R2/R5R6 γ values. As a result, we have no real constraint on the bias below 150 s. The solid curve was extrapolated down to 120 s, but we realize that the bias there may be even greater. Above 240 s, our attenuation values are in agreement with great circle studies, so the bias there is probably negligible. At all periods our corrected curve is within 1σ of the Mills and Hales [1977] estimate, although at periods below 200 s our mean γ is greater than theirs. A very recent study by Dziewonski and Steim [1982]

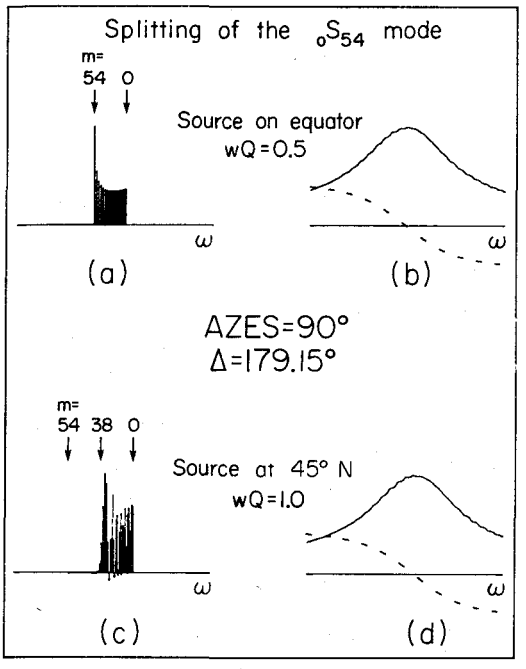

Fig. 10. Splitting of the peak $_0S_{54}$. (a) The frequencies and amplitudes of the singlets $_0S^m_{54}$, for a source located on the ellipsoid's equator and wQ=0.5. (b) The amplitude (solid line) and phase (dashed line) of the composite peak with attenuative broadening. (c) and (d) The corresponding results for a source at a latitude of 45° and wQ=1.0. The singlet amplitudes of Figure 10c are more irregular than in Figure 10a, but the composite peaks of Figures 10b and 10d are virtually identical except for a small frequency shift. See text for discussion.

supports our results down to 165 s, the minimum period of their analysis.

We mentioned earlier that the biasing effect shown in Figure 9 was independent of the orientation on the ellipsoidal earth model. We meant by this that Figure 9 would look the same if we changed either the event's strike or its location on the ellipsoid, while keeping the station at the proper distance and azimuth. Actually, if such changes were made, different values of the parameter wQ would be necessary to reproduce Figure 9 exactly. This would not affect our discussion of the allowable amount of bias in our measurements, which relied on the fact that the R1R2/R3R4 and R1R2/R5R6 curves split further apart as the bias increased. It does, however, affect our interpretation of the splitting width w as a measure of the earth's structural asymmetry. As it turns out, the value of w needed to induce a certain amount of bias is fairly insensitive to the event strike, and it varies as $(\cos^2\theta)^{-1}$ with the event latitude θ. For example, consider the results for wQ=0.5 in Figure 9, produced with the event on the ellipsoid's equator. If the event were moved to a latitude of 45°, we would require $wQ=0.5/\cos^2(45^\circ)=1.0$ in order to get the same results. Remember that all great circles through the event intersect at the antipode. With the event at latitude θ, the difference in path length between the longest and shortest great circles is

$$\delta L = 2\pi r_o\left(\frac{f}{2}\cos^2\theta\right) \simeq 2\pi r_o\left(w\cos^2\theta\right)$$

So the change in w needed to maintain a constant bias effect is just the change needed to keep constant the azimuthal variation in path length, or travel time, to the antipode.

Figure 10 demonstrates how the relationship between splitting width and event latitude affects the spectra of the peak $_0S_{54}$, which falls near the center of the 143- to 200-s period band. Figure 10a shows the singlet amplitudes $_0A^m_{54}$, for an event on the equator and wQ=0.5. Figure 10b shows the spectral amplitude and phase of the composite peak $_0S_{54}$. Below these, in Figures 10c and 10d, are the corresponding plots for an event at latitude 45° with wQ=1.0. The distributions of singlet amplitudes are markedly different for the two cases, but the shapes of the composite peaks are identical, consistent with the fact that in both cases attenuation measurements are biased by the same amount. In Figure 10a, the singlets are all of comparable amplitude, so that the spectral power is smeared fairly uniformly over the full width w. However, in Figure 10c the singlets m=40 to m=54 are very weak, so although the splitting width is nominally twice that of Figure 10a, the 'effective splitting width' is essentially the same.

One could now imagine a third case, that for the real earth. The singlets for the real earth would not show such a regular variation in eigenfrequency, and the amplitude distribution among them would be fairly random. But the composite peak for the real earth should look very much like, and result in time domain behavior very much like, the peaks of Figures 10b and 10d. This is the crucial assumption we have made in using results based on the ellipsoidal model to estimate the bias in real data.

To justify this assumption, we tested the effects of randomly perturbing the eigenfrequencies of the singlets within each mode peak. To do this, we first calculated the singlet amplitudes for the source-receiver geometry used in Figures 10c and 10d. As Figure 10c shows, the singlet amplitudes for this geometry scatter over a wide range of values. Each singlet was next assigned an arbitrary eigenfrequency within the range $(1\pm w/2)\omega_d$, using a random number generator. The singlet eigenfrequencies were generated independently for each mode $_0S_\ell$. The full spectrum in this random case was as a result even more pathological than for the real earth, for which one would expect the singlet pattern under $_0S_\ell$ to resemble that under $_0S_{\ell+1}$ (for $\ell >> 1$). We computed and analyzed time domain synthetics as before. The 'measured' attenuation curves for the random case behaved almost exactly like the curves of Figure 9. Individual curves oscillated slightly about the corresponding curves for the ellipsoidal model; the pattern of this oscillation changed for different sets of random eigenfrequencies. The important property of Figure 9 was reproduced identically: for comparable splitting widths, the R1R2/R3R4 and R1R2/R5R6 curves diverged from the input curve, and from each other, in the same fashion as in Figure 9. We conclude that this figure demonstrates an inescapable side effect of unresolved split mode peaks, an effect which is

independent of the singlet distributions beneath the peaks. The splitting widths and bias measures we have determined are not dependent upon the ellipsoidal model used to estimate them.

Discussion

In Table 1 we have compiled the results of the antipodal Rayleigh wave observations. The directly measured Q values, in the column labeled Q_o, are almost certainly biased due to the effects of a laterally heterogeneous velocity structure. These values establish a lower bound on global average Q values. The consistency of the R1R2/R3R4 and R1R2/R5R6 trends indicates that the bias can not be very large, or alternatively that the focusing at the antipode is quite sharp. The observed polarizations of the Rayleigh arrivals also support this conclusion. We have attempted to estimate the amount of bias using the consistency of the measurements as a constraint. The column of corrected Q values, Q_c, gives what we feel are the most reasonable global average Q consistent with the data, after removing the bias.

For periods below 250 s the corrected Q are still somewhat lower than the average values given in most conventional great circle studies. The corrected Q are, however, within the standard deviations given by Mills and Hales [1977]. The antipodal records we analyzed are of high quality, yielding stable, smoothly varying measurements of attenuation. They are also very consistent: radiation from the two events sampled the mantle in different ways, yet the results from the two events agree closely. Existing mantle attenuation models, such as SL2 of Anderson and Hart [1978] and that from the recent preliminary reference earth model (PREM) of Dziewonski and Anderson [1981], were constructed using the great circle results as constraints. In Figure 11 we compare the antipodal results to these two models. Model SL2 gives Q which are decidedly too high across the entire period band we have examined. The PREM model comes closer to the corrected antipodal Q but is still rather high at periods below 220 s. Above 280 s, the antipodal Q are possibly suspect due to very low signal amplitudes at these long periods. If the antipodal Q are indeed better global averages, then the upper mantle is more attenuative than has been generally recognized. Dziewonski and Steim [1982] have recently analyzed an extensive great circle data set to obtain high precision estimates of global Rayleigh wave attenuation down to periods of 165 s. From 280 to 165 s their results (see Table 1) are virtually identical to ours (average difference ~3%). This gives strong support to our method of correcting for bias. Further important information about the globally averaged attenuation profile in the mantle should be provided by antipodal recordings of the toroidal modes, lower-order Rayleigh modes, and the spheroidal overtones. We are in the process of collecting and analyzing such records.

In Table 1 we have also listed estimates of the splitting widths of the Rayleigh modes with periods between 120 and 250 s. Madariaga and Aki [1972] and Luh [1974] have calculated splitting widths of various modes for earth models with distinct continental and oceanic velocity profiles. Luh [1974] used the Canadian shield model CANSD [Brune and Dorman, 1963] for the continental structure and model 5-5-1 [Saito and Takeuchi, 1966] for the oceans. These models differ most significantly in the upper 120 km of the earth, with smaller differences extending to depths of 400 km. Luh [1974] calculated a splitting width for the mode ${}_0S_{40}$ (period = 212 s) of 0.32%. This compares favorably with our estimate of 0.29% for the splitting width at 210 s. The antipodal observations thus suggest that the differences between continental and oceanic structures are comparable to the differences between the CANSD and 5-5-1 models. Of course, greater variations may occur locally, but such variations are not important on a global scale.

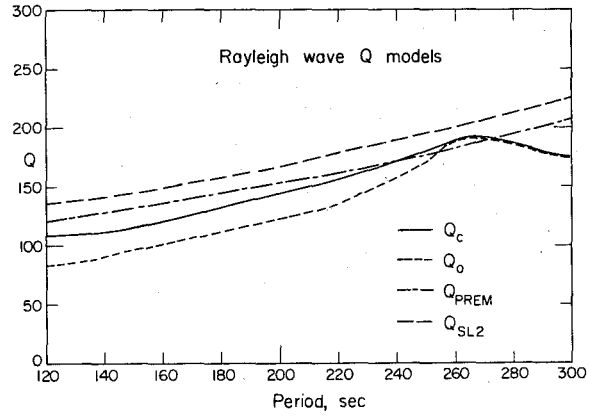

Fig. 11. Observed (Q_o) and corrected (Q_c) trends of the globally averaged Q of Rayleigh waves as a function of period, obtained from antipodal data. The attenuation models PREM and SL2 are shown for comparison.

Conclusions

The uncorrected antipodal results provide a lower bound for mantle Rayleigh wave Q values and, as such, provide an important constraint on absorption in the upper mantle. Because the 'stack' is complete we have attempted to estimate the bias due to lateral velocity heterogeneity and to correct the observed Q values for this effect. Although accounting for the effects of an unknown lateral heterogeneity may appear to be an intractable problem, we have confidence in our results for the following reasons:

1. The antipodal records give excellent agreement with previous great circle group velocity values.
2. The observed Rayleigh polarization indicates that focusing at the antipode is quite sharp.
3. Attenuation values are smooth, stable, and reproducible.
4. There is excellent consistency between successive passages of the Rayleigh wave groups.
5. Different events give almost identical results.
6. The method used to synthesize mode splitting allowed the heterogeneity to increase toward shorter periods.
7. The property used in estimating the bias, namely, the relative biasing of the R1R2/R3R4 and R1R2/R5R6 curves, is a general feature of mode splitting.
8. Our corrected attenuation values are in

TABLE 1. Results of Antipodal Rayleigh Wave Observations

T, s	U[a], km/s	Q_o[b]	Q_c[c]	$\delta\omega/\omega \times 100$[d]	Q_{DS}[e]	Q_{PREM}[f]	U_{PREM}[f]	T, s
120	3.75	83	108	0.37		122	3.72	120
130	3.72	86	109	0.36		125	3.70	130
140	3.69	91	112	0.35		128	3.68	140
150	3.67	97	116	0.34		132	3.67	150
160	3.64	101	121	0.34		136	3.65	160
170	3.62	106	127	0.33	135	140	3.63	170
180	3.61	111	132	0.32	138	144	3.62	180
190	3.60	120	138	0.31	140	148	3.60	190
200	3.59	123	143	0.30	146	153	3.59	200
210	3.58	128	150	0.29	150	157	3.58	210
220	3.58	134	155	0.28	156	162	3.57	220
230	3.58	146	164	0.27	160	166	3.57	230
240	3.58	157	170	0.27	166	171	3.57	240
250	3.59	170	180	0.26	172	176	3.58	250
260	3.60	188	188		179	182	3.59	260
270	3.61	192	192		185	188	3.62	270
280	3.63	187	187		190	194	3.64	280
290	3.66	179	179		198	200	3.68	290
300	3.70	176	176		204	207	3.73	300

[a]Group velocity, from Figure 3.
[b]From observed trend (dashed line) of Figure 6.
[c]From corrected trend (solid line) of Figure 6.
[d]Based on $wQ_{SL2} = 0.5$ ($\delta\omega/\omega = w$).
[e]Dziewonski and Steim [1982].
[f]Dziewonski and Anderson [1981].

excellent agreement with the most complete and precise recent studies.

9. Our estimates of the splitting widths due to lateral heterogeneity are consistent with previous studies.

Our uncorrected measurements of the attenuation coefficient γ lie, as they should, above previous estimates of global attenuation. The deviation increases at short periods which is consistent with the bias introduced by lateral heterogeneity in the upper mantle. Our uncorrected estimates of γ for periods greater than 200 s are lower than the Mills and Hales [1977] 'upper bound' (+1 standard deviation). Since our uncorrected estimates set lower bounds on Q, this indicates that the minimum Q of the mantle is more tightly constrained than before. Our corrected estimates of γ at shorter periods are at the upper end of the Mills and Hales [1977] estimated range, indicating that the Q of the shallow mantle is less than would be inferred from their estimate. Our corrected Q values, however, are within the stated errors ($\pm 1\sigma$) of the Mills and Hales [1977] data at all periods, and they agree with the Dziewonski and Steim [1982] data to within an average error of 3%.

Acknowledgments. We are indebted to Jose Rial, whose work with the antipodal body waves of the PTO record directly inspired this study. He introduced E.P.C. to the project and offered many valuable suggestions. We would also like to thank Tony Dahlen and Adam Dziewonski for pointing out the need to consider the bias in antipodal Q measurements. Ray Buland kindly provided mode tapes for model 1066A. Hiroo Kanamori and Jeff Given reviewed the manuscript and suggested improvements. We thank Adam Dziewonski and Joseph Steim for a timely preprint which lent support to our results. This research was supported by the National Science Foundation under contract EAR77-14675. E. P. C. was supported in part by a National Science Foundation graduate fellowship. Contribution 3644, Division of Geological and Planetary Sciences, California Institute of Technology, Pasadena, California 91125.

References

Anderson, D. L., and R. S. Hart, Attenuation models of the earth, Phys. Earth Planet. Inter., 16, 289-306, 1978.

Brune, J. N., and J. Dorman, Seismic waves and earth structure in the Canadian shield, Bull. Seismol. Soc. Am., 53, 167-210, 1963.

Dahlen, F. A., The spectra of unresolved split normal mode multiplets, Geophys. J. R. Astron. Soc., 58, 1-33, 1979a.

Dahlen, F. A., Exact and asymptotic synthetic multiplet spectra on an ellipsoidal earth, Geophys. J. R. Astron. Soc., 59, 19-42, 1979b.

Dziewonski, A. M., and D. L. Anderson, Preliminary reference earth model, Phys. Earth Planet. Inter., 25, 297-356, 1981.

Dziewonski, A. M., and J. M. Steim, Dispersion and attenuation of mantle waves through wave-form inversion, Geophys. J. R. Astron. Soc., in press, 1982.

Gilbert, F., and A. M. Dziewonski, An application of normal mode theory to the retrieval of structural parameters and source mechanisms from seismic spectra, Philos. Trans. R. Soc. London, Ser. A, 278, 187-269, 1975.

Jordan, T. H., and S. A. Sipkin, Estimation of the attenuation operator for multiple ScS waves, Geophys. Res. Lett., 4, 167-170, 1977.

Kanamori, H., Velocity and Q of mantle waves, Phys. Earth Planet. Inter., 2, 259-275, 1970.

Kanamori, H., and K. Abe, Deep structure of island

arcs as revealed by surface waves, Bull. Earthquake Res. Inst., Tokyo Univ., 46, 1001-1025, 1968.

Luh, P. C., Normal modes of a rotating, self-gravitating inhomogeneous Earth, Geophys. J. R. Astron. Soc., 38, 187-224, 1974.

Madariaga, R., and K. Aki, Spectral splitting of toroidal-free oscillations due to lateral heterogeneity of the earth's structure, J. Geophys. Res., 77, 4421-4431, 1972.

Mills, J. M., and A. L. Hales, Great-circle Rayleigh wave attenuation and group velocity, I, Phys. Earth Planet. Inter., 14, 109-119, 1977.

Mills, J. M., and A. L. Hales, Great-circle Rayleigh wave attenuation and group velocity, II, Phys. Earth Planet. Inter., 17, 209-231, 1978.

Nakanishi, I., Phase velocity and Q of mantle Rayleigh waves, Geophys. J. R. Astron. Soc., 58, 35-59, 1979.

Rial, J. A., On the focusing of seismic body waves at the epicentre's antipode, Geophys. J. R. Astron. Soc., 55, 737-743, 1978a.

Rial, J. A., Seismic waves at the epicentre's antipode, Ph.D. thesis, Calif. Inst. of Technol., Pasadena, 1978b.

Robinson, R., W. J. Arabasz, and F. F. Evison, Long term behavior of an aftershock sequence: The Inangahua, New Zealand, earthquake of 1968, Geophys. J. R. Astron. Soc., 41, 37-49, 1975.

Sailor, R. V., and A. M. Dziewonski, Measurements and interpretation of normal mode attenuation, Geophys. J. R. Astron. Soc., 53, 559-581, 1978.

Saito, M., and H. Takeuchi, Surface waves across the Pacific, Bull. Seismol. Soc. Am., 56, 1067-1091, 1966.

Sleep, N. H., R. J. Geller, and S. Stein, A constraint on the earth's lateral heterogeneity from the scattering of spheroidal mode Q^{-1} measurements, Bull. Seismol. Soc. Am., 71, 183-197, 1981.

(Received June 12, 1981;
revised January 22, 1982;
accepted January 29, 1982.)